ELSEVIER

S0032-3861(96)00164-4

Polymer Vol. 37 No. 16, pp. 3521–3530, 1996

0032-3861/96/$15.00 + 0.00

Poly(ether urethane)/poly(ethyl methacrylate) interpenetrating polymer networks: morphology, phase continuity and mechanical properties as a function of composition

Douglas J. Hourston* and Franz-Ulrich Schäfer
Institute of Polymer Technology and Materials Engineering, Loughborough University, Loughborough, Leicestershire LE11 3TU, UK
(Received 29 August 1995; revised 20 December 1995)

The composition range of polyurethane (PUR)/poly(ethyl methacrylate) (PEMA) interpenetrating polymer networks was investigated with respect to morphology and phase continuity using mechanical and dynamic mechanical methods and transmission electron microscopy (TEM). Dynamic mechanical data revealed one main tanδ transition with a shoulder for the intermediate compositions from 70:30 to 40:60 indicating a semi-miscible system. For the remaining compositions only one peak, indicating a higher degree of miscibility was observed. The storage and elastic moduli were related to the Davies, Kerner and Budiansky modulus–composition models. The Budiansky modulus–composition model, which indicates phase inversion at the mid-range composition, resulted in the best fit. However, it was found that the shape of the modulus *versus* composition curves was strongly temperature-dependent. In previous studies, not much attention had been given to the temperature at which the modulus–composition studies were conducted. Tensile testing revealed a strong synergistic effect at the 70:30 PUR/PEMA composition with maxima occurring at this composition for both the elongation at break and the toughness index. The tensile strength increased in a three-step regime corroborating the dynamic mechanical thermal analysis results. TEM micrographs confirmed a co-continuous system at the 70:30 to 40:60 PUR/PEMA mid-range compositions.

(Keywords: interpenetrating polymer networks; polyurethane; poly(ethyl methacrylate))

INTRODUCTION

It is often important to know the morphology of multicomponent polymer systems, and the factors influencing it, since phase domain size and shape, interfacial bonding and phase connectivity determine the physical and mechanical properties of such materials[1,2]. Interpenetrating polymer networks (IPNs) are a class of polymer blend[1,2] with very special properties. Full IPNs are characterized by the presence of crosslinks in both polymers which control the average phase domain size. The morphology of IPNs is particularly complicated and has been subject to many studies[1–5]. During polymerization, two competing processes take place simultaneously. Phase separation of the forming polymer chains proceeds by diffusion through an increasingly viscous medium to form phase domains. The formation of crosslinks restricts diffusion and, at gelation, the then present situation is frozen in. Consequently, phase separation in IPNs depends[2,3] primarily on: (i) the miscibility of the constituent polymers; (ii) the crosslink density in both polymer networks and inter-network grafting; (iii) the reaction conditions (temperature, pressure), i.e. the reaction mixture viscosity; and (iv) the relative reaction rates of network formation. With highly incompatible polymers, the thermodynamic driving force for phase separation is so powerful that gross phase separation occurs before gelation. Yet, with semi-compatible polymer pairs, IPNs with a very fine microheterogeneous morphology[4] possessing phase domains in the order of 5–30 nm can be obtained. Among the techniques that have been used to investigate IPN morphology are transmission[6,7] (TEM) and scanning[8] (SEM) electron microscopy, dynamic mechanical analysis[9], modulus–composition studies[10,11], small-angle neutron scattering[12,13], small-angle X-ray scattering[14,15] and dielectric measurements[16].

In the present study, the morphology of polyurethane (PUR)/poly(ethyl methacrylate) (PEMA) IPNs of varying composition was investigated. Both polymers contain groups which are polar to a certain extent and their solubility parameters, determined[17] by equilibrium swelling, are 20.3 $(J\,cm^{-3})^{1/2}$ for the PUR and 18.0 $(J\,m^{-3})^{1/2}$ for the PEMA. Special focus was placed on the phase continuity since the latter strongly influences the mechanical properties of the polymer

* To whom correspondence should be addressed

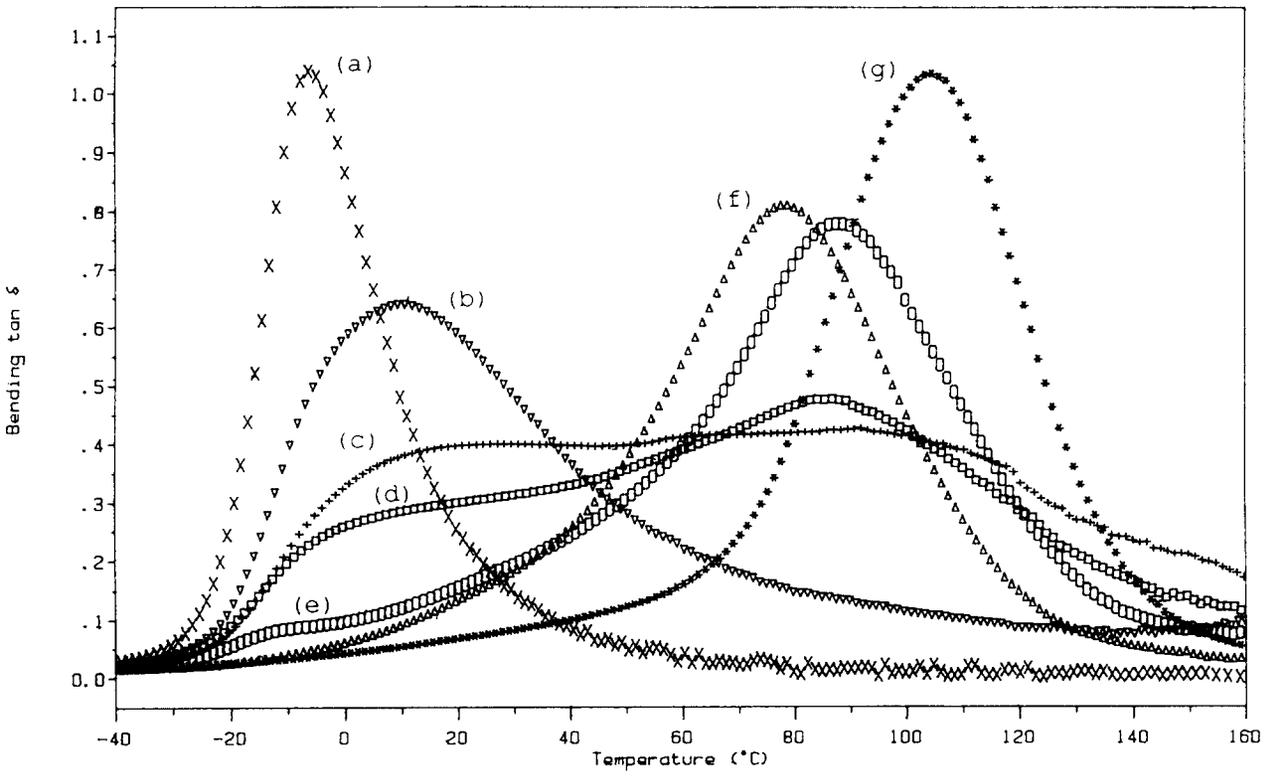

Figure 1 Loss factor versus temperature for the PUR/PEMA IPN compositions. (a) 100% PUR; (b) 80:20 PUR/PEMA IPN; (c) 70:30; (d) 60:40; (e) 40:60; (f) 30:70; (g) 100% PEMA

blend. Amongst the factors determining the phase continuity[1,18,19] in polymer blends are the volume fractions and viscosities of each component. The relative rates of formation of the networks are particularly important in IPNs. The network that forms first[20], and/or the one with the higher crosslink density[6], is likely to represent the continuous phase. The damping ability of a range of PUR/PEMA IPNs was shown in an earlier publication[17] in terms of loss modulus and loss factor *versus* temperature data. At the 70:30 PUR/PEMA IPN composition, a very broad transition range spanning 130°C where the tanδ values were greater than 0.3 and a high value for the area under the linear loss factor curve (TA) of 62.1 K were obtained. In the present study, these loss curve data are interpreted in terms of morphology, i.e. phase continuity and miscibility of the polymer components. Further, mechanical studies such as tensile testing and hardness measurements were conducted. The storage and the elastic moduli were compared with modulus–composition theories to predict dual-phase continuity and phase inversion. TEM was used to corroborate the findings from the mechanical tests.

EXPERIMENTAL

Materials

Poly(oxypropylene glycol) of a molar mass of 1025 (PPG1025, supplied by BDH) was used as the polyurethane (PUR) soft segment. The hard segment was formed from the 1,1,3,3-tetramethylxylene diisocyanate (m-TMXDI, kindly donated by Cytec) and the crosslinker trimethylol propane (TMP, supplied by Aldrich). Stannous octoate (SnOc, supplied by Aldrich) was used as the PUR catalyst. Poly(ethyl methacrylate) (PEMA) was formed by crosslinking ethyl methacrylate monomer (EMA, supplied by Aldrich) with tetraethyleneglycol dimethacrylate (TEGDM, supplied by BDH). Azoisobutyronitrile (AIBN, supplied by BDH) was used as the initiator.

IPN preparation

The IPN preparation[6] has been described in an earlier publication. In brief, the TMP was dissolved in the PPG1025 at 60°C. At room temperature, the polymer component mixture, which included the EMA, TEGDM and the dissolved AIBN, was added. Upon addition of the SnOc and the TMXDI, the components were stirred under a nitrogen blanket for 5 min. After degassing for 1 min at high vacuum, the mixture was moulded[6] in an O-ring mould. Curing was conducted in 3 cycles of 24 h at 60, 80 and 90°C.

Dynamic mechanical thermal analysis

Dynamic mechanical thermal analysis (d.m.t.a.) measurements were conducted with a Polymer Laboratories MKII instrument in the single cantilever bending mode. The temperature programme was run from −60 to 200°C using a heating ramp of 3°C min^{-1} at a fixed frequency of 10 Hz. The applied strain setting was ×4.

Tensile testing

Stress–strain analyses were conducted using a Lloyd 2000R instrument equipped with a 500 N load cell. A crosshead speed of 50 mm min^{-1} was chosen. Small size dumb-bells with a gauge length of 30 mm were used in this study. Tests were conducted at room temperature of

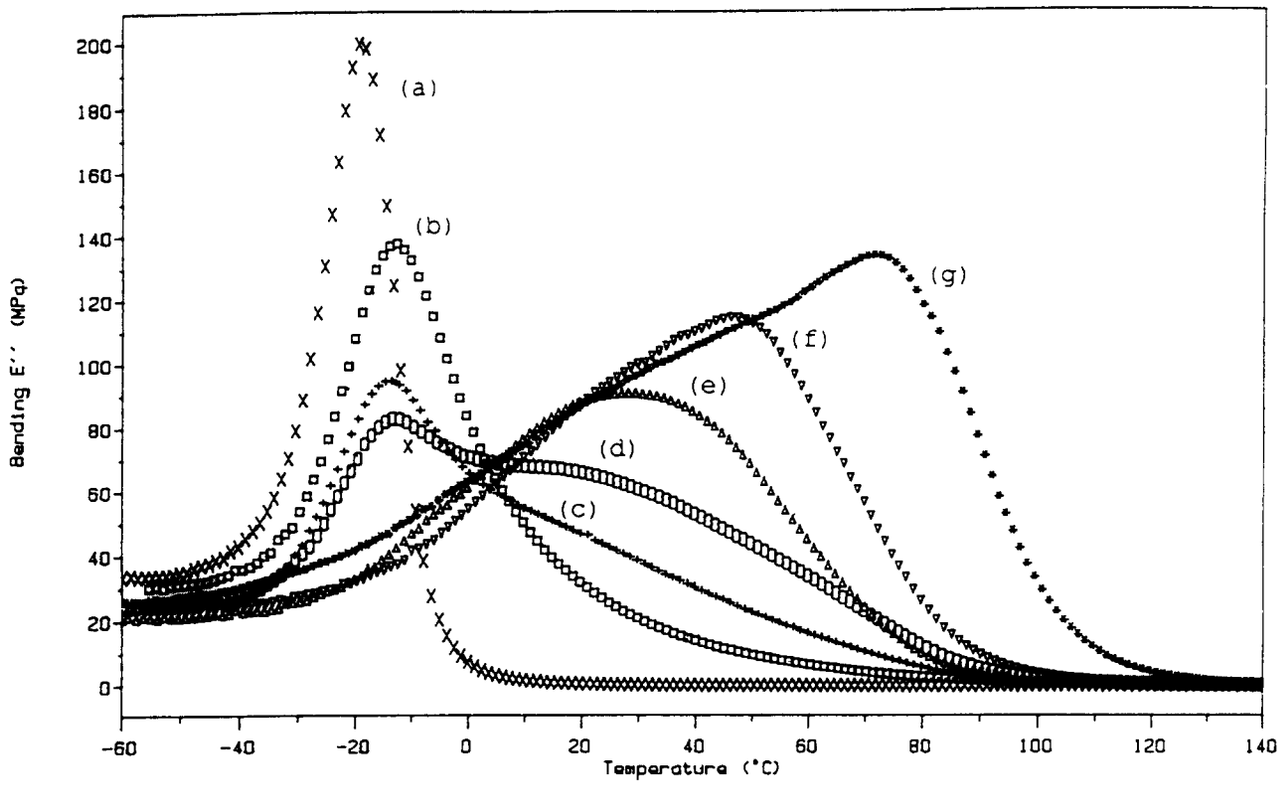

Figure 2 Loss modulus *versus* temperature data for the PUR/PEMA IPN compositions. (a) 100% PUR; (b) 70:30 PUR/PEMA IPN; (c) 50:50; (d) 40:60; (e) 30:70; (f) 20:80; (g) 100% PEMA

23 ± 1°C and the values quoted are an average of 4–5 samples.

Hardness measurements

Shore A hardness was determined using a Zwick model 3114, whilst Shore D values were evaluated using a Jamaica Instruments gauge. The tests were again conducted at room temperature (23 ± 1°C). The hardness values quoted are an average of eight readings taken at random over the entire specimen surface.

Transmission electron micrographs

The elastomeric samples were embedded in epoxy resin and ultra-microtomed into 100-nm thick sections. Staining was conducted for 48 h in a 2 wt% osmium tetroxide solution. The electron micrographs were taken with a Jeol Jem 100 CX instrument using an accelerating voltage of 60 kV.

RESULTS AND DISCUSSION

Dynamic mechanical data can be used to study the morphology, i.e. the phase continuity and the miscibility of a polymer blend. The plot of the storage modulus at a given temperature *versus* composition can be related to models which allow predictions about phase continuity

Table 1 Dynamic mechanical and mechanical properties of the PUR/PEMA IPN composition series

Composition (wt% PUR)	D.m.t.a. (10 Hz) T_g (tanδ °C^{-1}) PUR/PEMA	Ultimate tensile properties: Stress at break (MPa)	Elongation at break (%)	Young's modulus (MPa)	Toughness (J)	Hardness shore A
100	−5	1.2	210	1.0	0.60	40
90	3	1.4	280	1.3	1.1	41
80	10	4.2	410	3.3	2.7	46
70[a]	18/87	9.3	360	8.0	7.5	74
60[a]	10/87	9.6	230	39	4.6	85
50[a]	−10/27/88	10	110	70	3.7	94
40[a]	−12/88	13	75	210	3.7	98
30	79	12	44	300	2.5	99
20	85	18	22	500	1.8	99
10	95	32	12	770	1.1	99
0	105	45	9.8	870	0.9	99

[a] T_gs at these compositions were difficult to determine because of the presence of a significant shoulder for the second component

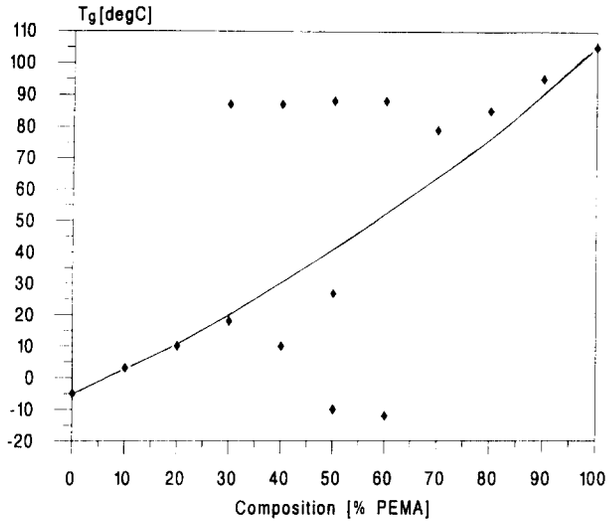

Figure 3 T_gs taken from the tanδ maximum at 10 Hz (◆) *versus* composition data. The line represents the prediction of the Fox equation

and phase inversion in a polymer blend to be made. In the tanδ *versus* temperature plot, one narrow loss factor peak indicates a high degree of miscibility, whereas two clearly separated tanδ transitions with low inter-transition tanδ values are indicative of gross phase separation. The intermediate situation of one broad transition is obtained for semi-miscible polymer blends. Generally, two loss factor peaks of equal height can be an indication[21] of dual-phase continuity.

The linear loss factor and linear loss modulus *versus* temperature data for both homonetworks and selected IPN compositions are shown in *Figures 1* and *2*. Both data sets have been shown for the entire composition series in an earlier publication[17], where they were only discussed in terms of the areas, *TA* and *LA*, under the respective linear curves. The glass transition temperatures (T_gs), as obtained from the loss factor peak at 10 Hz, are presented in *Table 1*. A single transition peak in the loss factor *versus* temperature data was observed for the 90:10, 80:20, 30:70. 20:80 and 10:90 IPN compositions. The intermediate compositions between 70:30 and 40:60 were phase-separated to some extent and exhibited a shoulder for the second transition. The fact that the T_g for the PUR shoulder at the 50:50 and 40:60 PUR/PEMA compositions was even lower than that of pure PUR network can be explained by a plasticization effect[22] and, probably more importantly, by an incompetently formed PUR network[23] containing defects such as loose chain ends. The 50:50 composition shows three transitions, one main peak at 88°C with two shoulders at 27°C and −10°C. A similar phenomenon has been reported[22–24] previously for PUR/poly(methyl methacrylate) (PMMA) IPNs and was explained by the presence of a substantial interphase region. *Figure 3* shows a plot of T_g *versus* composition compared with the Fox equation[25].

The Fox equation predicts a concave curve for T_g *versus* composition. This equation is given as $1/T_g = M_1/T_{g1} + M_2/T_{g2}$, where the subscripts 1 and 2 refer to the two polymers, M is the weight fraction and T_g is in absolute temperature units. Only the data points for the 90:10, 80:20 and 70:30 PUR/PEMA IPNs are in line with the prediction. Even though only a single T_g was obtained for the IPNs containing 70, 80 and 90% PEMA, a fit with the Fox equation did not result. The mid-range composition would not be expected to fit

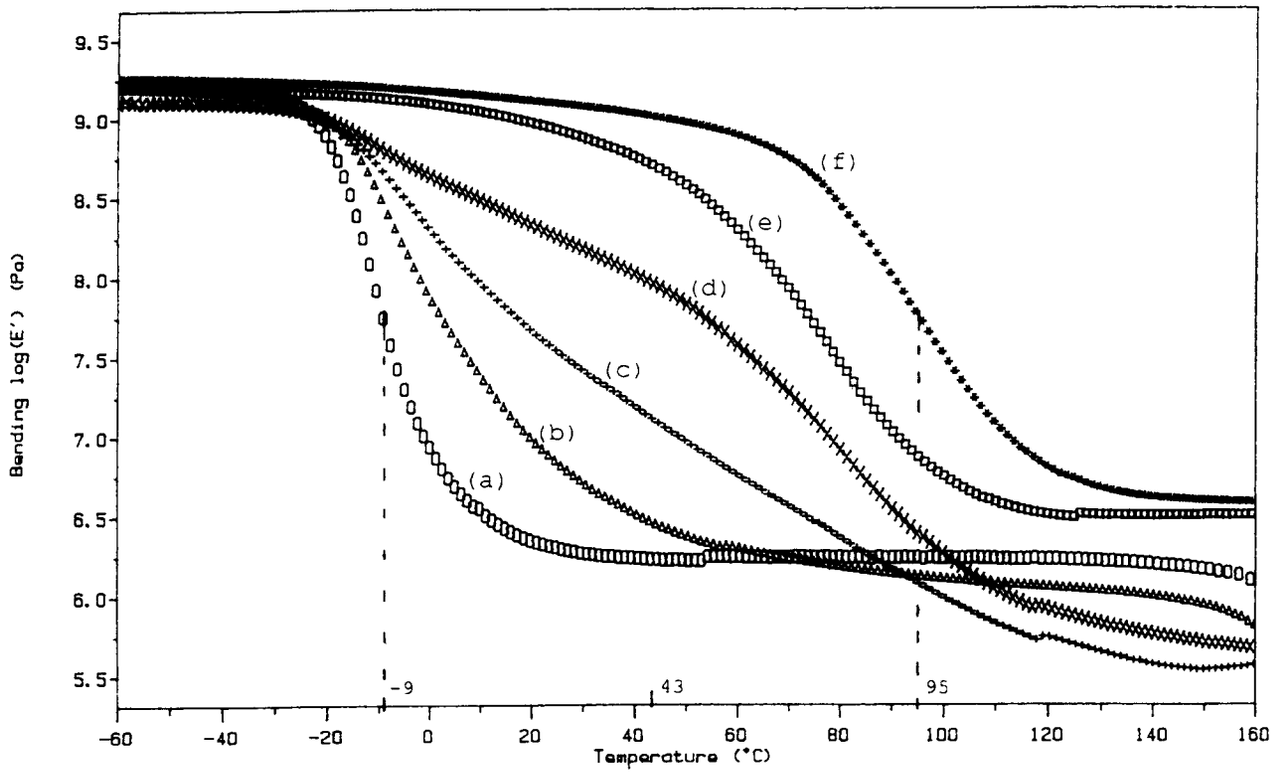

Figure 4 Storage modulus *versus* temperature data for the PUR/PEMA IPN compositions. (a) 100% PUR; (b) 80:20 PUR/PEMA IPN; (c) 70:30; (d) 50:50; (e) 20:80; (f) 100% PEMA

the prediction, since unsymmetrical transitions with shoulders were obtained. Yet, no gross phase separation took place, which can be seen from both the inward shift of the transition peaks and the high inter-transition tanδ values. The location of the linear loss modulus peak changes only marginally up to the 30:70 PUR/PEMA IPN composition (*Figure 2*). Yet, at this composition a major change in curve shape and peak shift to higher temperatures can be seen.

Phase continuity can also be studied by relating the dynamic storage modulus, E', to theoretical modulus–composition models. The E' *versus* temperature data for selected IPN compositions are shown in *Figure 4*. From this data, it appears that the PUR/PEMA IPNs possess a semi-miscible morphology. The storage moduli do not decrease in a clear-cut two-step manner, which would be indicative of two-phase polymer blends. For the 70:30 composition, for example, E' steadily decreases until it reaches the rubbery plateau. The storage modulus in the rubbery plateau is highest for the pure PEMA network. The latter is crosslinked with 5 mol% TEGDM which amounts to a theoretical average molar mass between crosslinks ($M_{c,t}$) of 1250 g mol^{-1}. The lower E' of the rubbery plateau for the pure PUR network can be explained because of a higher $M_{c,t}$. A diol/triol ratio of 3:1 results in a $M_{c,t}$ of 2870 g mol^{-1}. Surprisingly, intermediate compositions such as the 70:30 and the 50:50 IPN exhibited even lower storage moduli in the rubbery plateau region than either of the two homonetworks. This is indicative of a lower apparent crosslink density in these IPNs. This might be explained on the grounds that when both networks are continuous they impede the complete formation of the other. Incomplete formation of the PUR was already suspected from the T_g data.

Several theories have been developed[10,26] to relate the modulus of a multiphase system to its composition and morphology. Most theories assume perfect adhesion between the phases and the sample being macroscopically homogeneous and isotropic. Kerner[27] derived a theory for a matrix with spherical inclusions.

$$G/G_1 = [(1 - \phi_2)G_1 + (\alpha + \phi_2)G_2]/$$

$$[(1 + \alpha\phi_2)G_1 + \alpha(1 - \phi_2)G_2] \quad (1)$$

Here, subscripts 1 and 2 refer to the matrix and the inclusions, respectively. G is the shear modulus, ϕ is the volume fraction and α is a function of the matrix Poisson ratio, $\nu_1 : \alpha = 2(4 - 5\nu_1)/(7 - 5\nu_1)$. Davies[28,29] proposed the following relation which is designed for systems in which both components are present as continuous phases.

$$G^{1/5} = \phi_1 G_1^{1/5} + \phi_2 G_2^{1/5} \quad (2)$$

A model which predicts phase inversion at mid-range compositions in two-phase polymer systems was developed by Budiansky[30].

$$\phi_1/(1 + \epsilon(G_1/G - 1))$$

$$+\phi_2/(1 + \epsilon(G_2/G - 1)) = 1 \quad (3)$$

Again, ϕ is the volume fraction, ϵ equals $2(4 - 5\nu)/15(1 - \nu)$, ν is Poisson's ratio of the composite, G is the shear modulus and subscripts 1 and 2 represent the component polymers. Conversion from the shear to the tensile modulus, E, was conducted using equation $E = 2G(1 + \nu)$. The Poisson's ratios, ν, for the homopolymers, were assumed to be 0.5 for the polyurethane and 0.35 for the PEMA[31], and the Poisson's ratios for the compositions were calculated using the linear rule of mixing[31].

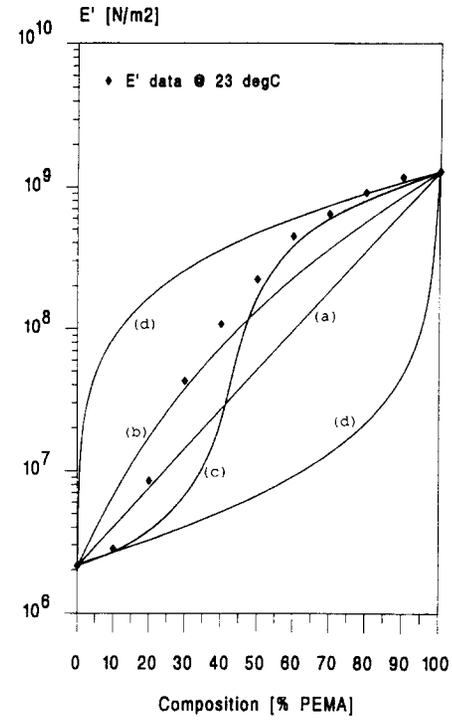

Figure 5 Storage modulus *versus* composition data compared with modulus–composition models. (◆) Storage modulus data (23°C, 10 Hz). (a) The logarithmic rule of mixing; (b) the Davies equation; (c) the Budiansky equation; (d) the upper and lower bounds of the Kerner equation

So far, the fit of experimental data to modulus–composition theories has been contradictory. Hourston and Zia[32] found the Davies equation to fit their data well for simultaneous semi-II PUR/PMMA IPNs. For semi-II PUR/poly(methyl acrylate) (PMA) IPNs[33], a close fit by the Davies equation was obtained by changing the exponent to 1/10. A PUR/poly(vinyl acetate) (PVAc) semi-I IPN series fitted the Davies equation well[33], when the exponent was altered to 1/6. They reasoned that this was an indication for a better miscibility in the semi-I PUR/PVAc system than in the semi-II PUR/PMA IPN. Good fits with the Davies equation were also obtained by Allen *et al.*[10] for PUR/PMMA and PUR/poly(acrylonitrile) IPNs. Akay and Rollins[9] compared the modulus *versus* composition plots of simultaneous and sequential PUR/PMMA IPNs. They found the elastic modulus–composition plots to comply with Budiansky's phase inversion model for simultaneous IPNs and with a dual-phase continuity model (Davies equation) for sequential IPNs. The dynamic storage moduli, however, behaved according to the Davies equation. For other simultaneous full and semi PUR/PMMA IPNs, Kim *et al.*[31] found a fairly good fit with the Budiansky equation. The fit was better for the Young's modulus *versus* composition data than for the respective shear modulus *versus* composition data, a fact that was attributed to experimental errors. In

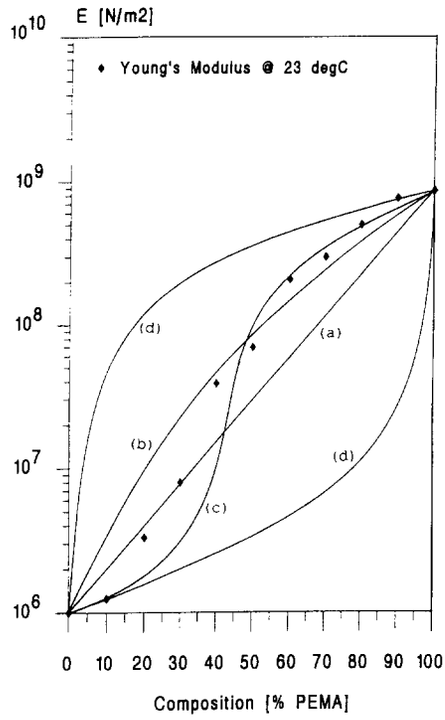

Figure 6 Young's modulus *versus* composition data compared with modulus–composition models. (◆) Young's modulus data (23°C). (a) The logarithmic rule of mixing; (b) the Davies equation; (c) the Budiansky equation; (d) the upper and lower bounds of the Kerner equation

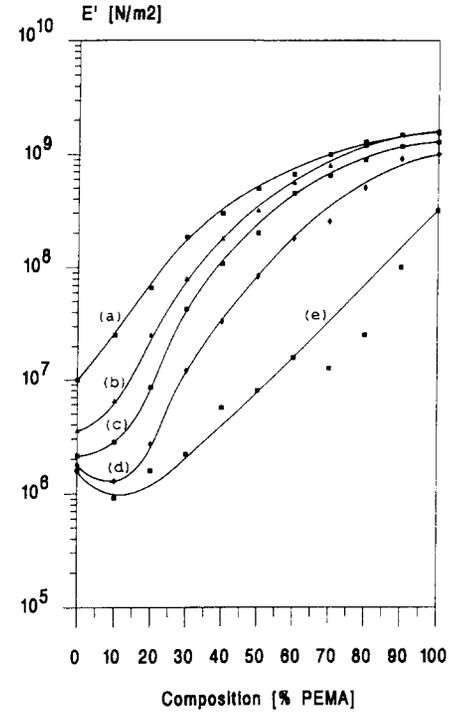

Figure 7 Storage modulus *versus* composition data taken at different temperatures. (a) E' data at 0°C; (b) at 10°C; (c) at 23°C; (d) at 43°C; (e) at 80°C. The solid lines are the best fit through the data points

most of these studies, however, the conclusions drawn were based on three or four composition points[34] which makes it difficult to make predictions over the whole composition range. Therefore, in the present study, the entire composition range was prepared in 10 wt% increments. The dynamic storage moduli (10 Hz) at 23°C of the IPNs and of the homonetworks are plotted against the composition in *Figure 5*. The experimental data points for the storage modulus do not fit exactly any of the theoretical models investigated. However, clearly the shape of the Budiansky equation, involving phase inversion at the intermediate composition, gives the best approximation. From the data for this simultaneous PUR/PEMA IPN, phase inversion seems to take place at the 80:20 composition. The Young's modulus obtained from tensile testing at room temperature is shown *versus* composition in *Figure 6*. In contrast to Akay and Rollins[9], who observed different trends for the elastic modulus and the dynamic storage modulus, with the former following the Budiansky and the latter the Davies equation, in the work now being reported, the curve shapes of Young's modulus *versus* composition are very similar to those of the dynamic storage modulus *versus* composition. The values for the latter are higher than the Young's modulus counterparts, which is explained by the frequency effect. Phase inversion seems to take place at a slightly higher PEMA weight fraction, namely at the 70:30 composition. An important factor that has been neglected so far in modulus–composition studies is the temperature at which the investigation is conducted. Because of its practical importance and convenience for tensile testing, most modulus–composition studies have been conducted using room temperature data, irrespective of the T_gs of the constituent polymers. The fact that temperature might have an influence on the shape of the modulus–composition curve was experienced in *Figures 5* and *6*. The dynamic storage modulus seems to have its phase inversion at a lower weight fraction (20% PEMA) than the one from the elastic modulus which is at 30%. Since in dynamic experiments frequency is equivalent to temperature, it seems that by conducting modulus–composition studies closer to the T_g of the lower T_g component, phase inversion is apparently shifted to lower weight fractions of polymer 2. In order to confirm this assumption, plots of storage modulus *versus* composition were made at 0°C, 10°C, 23°, 43°C and 80°C (*Figure 7*). These temperatures were chosen because one (0°C) was near the T_g of the PUR network (−5°C from tanδ peak) and 80°C was relatively near the PEMA network T_g (105°C). The temperatures of the half-step drop of the pure PUR network (−9°C) and of the pure PEMA network (95°C) storage moduli were determined in *Figure 4*. The temperature intermediate between these two points (43°C) was chosen for this modulus–composition study. The five curves in *Figure 7* clearly confirm the above idea. Conducting the modulus–composition studies at temperatures near to the lower T_g polymer results in an apparent phase inversion at lower weight fractions of the higher T_g polymer (*Figures 7d–7b*). An extreme case is shown in *Figure 7a*, where no phase inversion appears to be occurring with the curve resembling the Davies equation for dual-phase continuity. At the other extreme of 80°C, the curve is of a concave shape. Thus, altering the 1/5 exponent from the Davies equation to a value for the exponent n of $0 > n > -1$ and introducing it into Nielson's general mixing equation[26,35]

$$P^n = \phi_1 P_1{}^n + \phi_2 P_2{}^n \quad (4)$$

where P stands for a given property of the two-phase

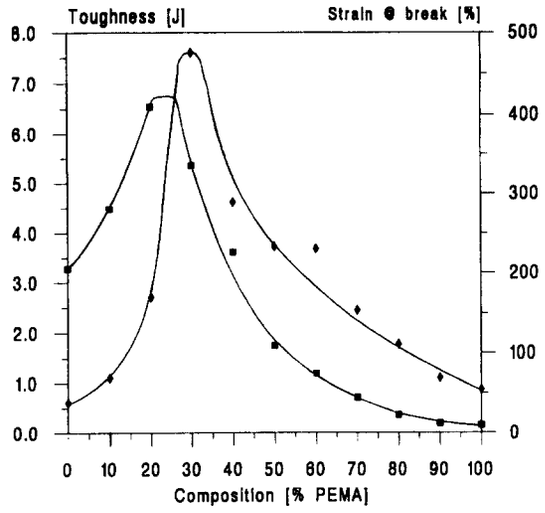

Figure 8 Tensile testing results *versus* composition for the PUR/PEMA IPNs and homonetworks. ■, Strain at break; ◆, toughness index

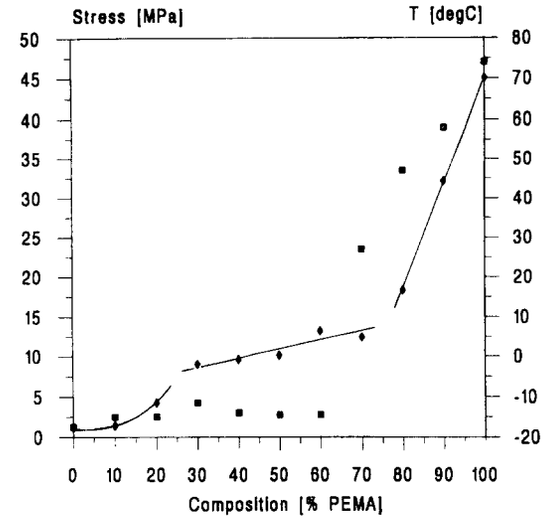

Figure 9 Stress at break (◆) and location of the linear E'' peak (■) *versus* composition for the PUR/PEMA IPNs and homonetworks

composite, would yield a similar concave curve shape. Between these two extremes, intermediate curve shapes can be obtained at different temperatures. The irregularities, particularly in the curve at 80°C, changing from the 40:60 to the 30:70 composition are due to a difference in miscibility/morphology of the IPN which has already been shown in *Figures 1* and *3* and *Table 1*. The same irregularities can be seen, to a lesser extent, in the modulus–composition study at 43°C. At this intermediate temperature between the half-step drop of the homonetwork storage moduli, phase inversion seems to take place at the 70:30 composition. This further corroborates the finding of co-continuous phases which had already been indicated by the equal tanδ peak heights in the d.m.t.a. data (*Figure 1*). The fact that the Young's modulus *versus* composition plot predicted, correctly, the phase inversion to take place at the 70:30 composition was because this modulus is acquired from a static test. T_gs obtained from differential scanning calorimetry (d.s.c.) measurements for both homonetworks happened to be approximately 20°C lower, so that room temperature was very close to the intermediate temperature. Thus, it can be concluded that contradictory results might have arisen because of an insufficient number of composition data points and disregard of the effect of the temperature on the test results.

The strain at break and toughness index from tensile test are shown in *Figure 8* for the PUR/PEMA IPNs. For both the strain at break and the toughness index, a true synergistic effect was observed, with the optimum IPN composition surpassing, by far, either of the two homonetworks. These special properties were both obtained around the 70:30 PUR/PEMA composition. This might be explained by the fact that both networks were continuous and that network interpenetration was achieved on a high level. The largest elongation at break (410%) was twice as high as that of the pure PUR network. The location of the highest elongation at break at the 70:30 composition coincides with that of the lowest storage modulus in the rubbery region at 140°C (*Figure 2*). Again, this is an indication of a lower apparent crosslink density in the IPN and indicates that both networks did prevent each other from developing fully.

The toughness index for the 70:30 PUR/PEMA IPN at 7.5 J was more than seven times as high as either of the homonetwork values. This corroborates the findings from the loss factor *versus* temperature data where the highest area under the linear loss factor curve was found[17] for this composition (*Figure 2*). Thus, this composition possesses very good energy absorbing characteristics.

So far, the 70:30 composition has been found to have outstanding properties. Here, a change in the phase continuity from a predominantly PUR matrix to a co-continuous structure was found to occur. Data in *Figure 9* may indicate over what composition range this dual phase continuity extends.

The stress at break and the location of the linear loss modulus peak are plotted *versus* the IPN composition. The values for the stress at break show three distinctive regions. The first three values for the 100:0, the 90:10 and the 80:20 compositions are very low. From d.m.t.a. data, it was noted that at these compositions it was the PUR network that constitutes predominantly the matrix. A two-fold increase to around 10 MPa was found for the 70:30 composition. This value then remains fairly constant over the entire mid-range composition, increasing only slowly to above 13 MPa for the 30:70 IPN. This second region with only gradually increasing stress at break values might indicate that at these mid-range compositions a co-continuous morphology is present. For the 20:80 to the 0:100 compositions, a rapid increase in the stress at break values up to 45 MPa for the pure PEMA network was found. This is an indication of a further change in the IPN morphology to an increasingly predominant PEMA matrix, with very little or no continuity of the PUR network. The latter finding was corroborated by the linear loss modulus peak locations. The loss modulus, E'', is the product of the storage modulus and the loss factor. For both, their location and magnitude depend strongly upon the miscibility and connectivity of the polymer components. For a completely miscible polymer blend, the location of the linear E'' peak would move increasingly to higher

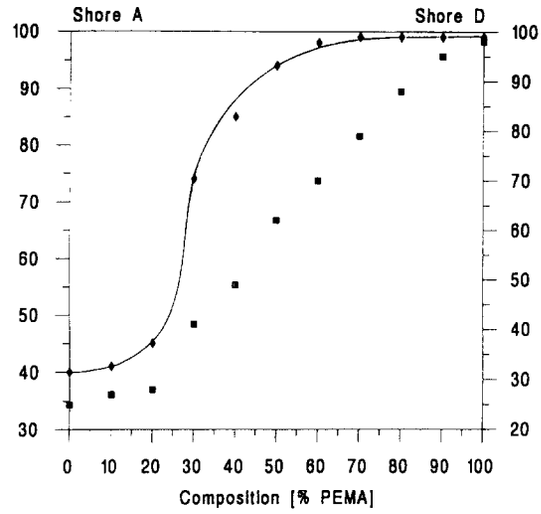

Figure 10 Shore A hardness (◆) and Shore D hardness (■) *versus* composition for the PUR/PEMA IPNs and homonetworks

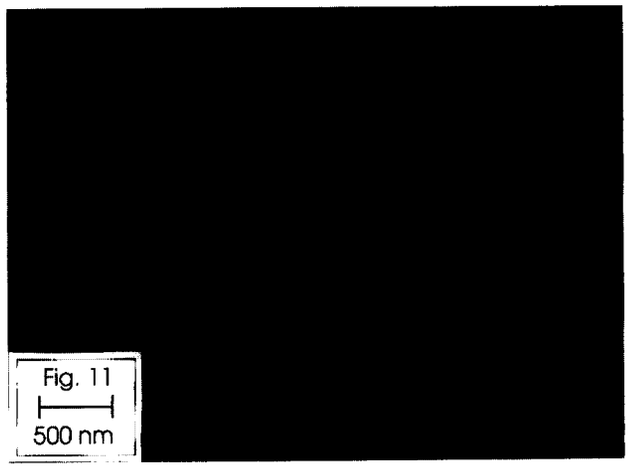

Figure 11 TEM micrograph of the 70:30 PUR/PEMA IPN

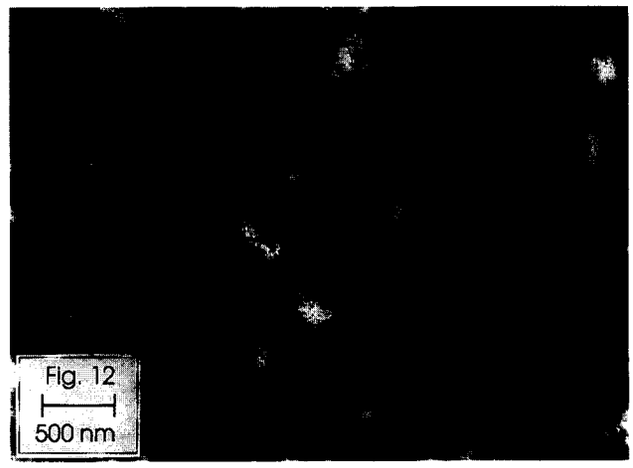

Figure 12 TEM micrograph of the 50:50 PUR/PEMA IPN

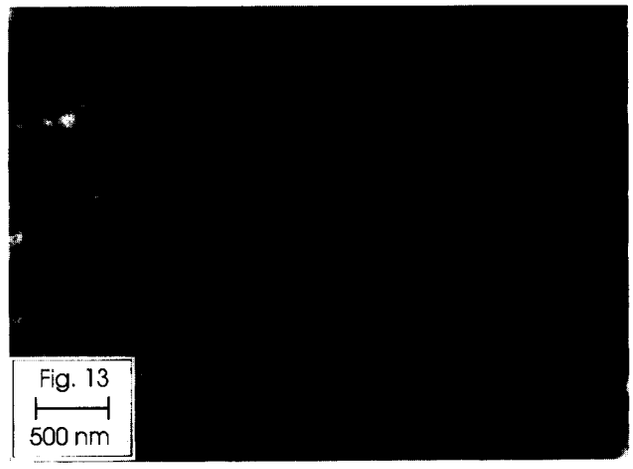

Figure 13 TEM micrograph of the 40:60 PUR/PEMA IPN

temperatures with increasing fraction of the higher T_g polymer. In this semi-miscible PUR/PEMA IPN, a different pattern was observed. The loss modulus peak location remained very much unchanged up to around 70 wt% PEMA. At this composition, a major E'' peak shift towards higher temperatures occurred. This is a strong indication that the properties of the IPN are now to a great extent determined by a continuous PEMA phase with discontinuous PUR domains dispersed in it. At lower PEMA compositions, the PUR component still influences the IPN properties significantly, and is thus thought to be continuous to some degree.

The Shore A indentation hardness *versus* composition curve shown in *Figure 10* (data in *Table 1*) agrees completely with the modulus behaviour in *Figures 4* and *5*. A considerable increase in Shore A hardness was found for the 70:30 PUR/PEMA composition which indicated a change in the continuous phase. This similar behaviour would be expected since the hardness is directly related to modulus, strength and elasticity[36,37]. For Shore D hardness values, a linear pattern was found for an increase in PEMA content. It must, however, be emphasized that the data obtained at the outer ranges are not very reliable. The useful range was indicated[38] to be between 10 and 90 for Shore A and between 30 and 90 for Shore D. Thus, the phase inversion at the 70:30 composition was below the useful operating range of Shore D.

TEM micrographs of the different compositions corroborated the findings from the dynamic mechanical investigations. For all compositions, no gross phase separation was observed. The phase domains were not well defined, but show a gradual change in composition. The 90:10 and the 80:20 PUR/PEMA IPNs were difficult to ultramicrotome because of their softness at room temperature. The micrographs showed a very fine morphology with white PEMA domains in the order of 5–40 nm in a dark OsO_4-stained PUR matrix. For the 70:30 PUR/PEMA IPN composition (*Figure 11*), white interconnected domains of PEMA in a dominant PUR matrix were observed.

Thus, dual phase continuity was also confirmed by TEM microscopy. With an increasing amount of PEMA, the white phase became more dominant. At the 50:50 PUR/PEMA composition (*Figure 12*), interconnected PUR and PEMA phases were present to an equal extent.

A suprastructure which exhibited phase domains in the range 100–500 nm was observed. Also, a finer structure which in most cases could be described as PUR domains within PEMA domains within a PUR matrix was observed. Here, very small phase domains of

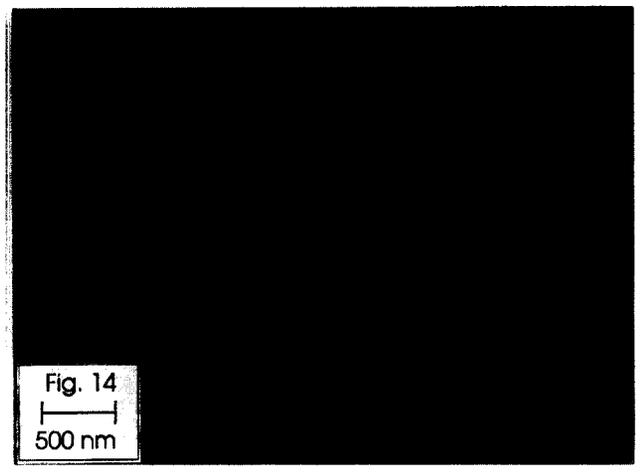

Figure 14 TEM micrograph of the 30:70 PUR/PEMA IPN

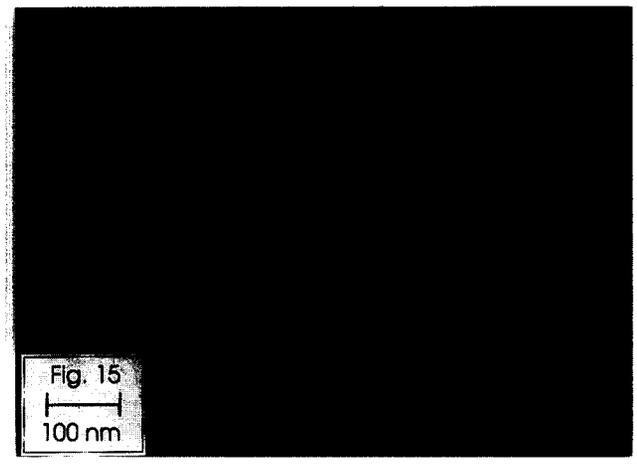

Figure 15 TEM micrograph of the 20:80 PUR/PEMA IPN

5–50 nm were noted. The latter structure might be responsible for the third transition that was observed in the loss factor *versus* temperature curve at the 50:50 composition. At the 40:60 PUR/PEMA composition (*Figure 13*), both phases still appeared to be co-continuous.

However, a general trend towards a PEMA matrix with 50–300 nm dispersed PUR domains was observed. At the 30:70 composition, a change in the properties to a predominantly PEMA-dominated profile was found in the mechanical tests. The micrograph of this composition (*Figure 14*) showed fairly small (5–50 nm) PUR domains in a PEMA matrix, which is in good agreement with the observations made from the mechanical tests. At the 20:80 composition (*Figure 15*), the PUR phase domains were only just resolvable by TEM. The PUR domains were in the order of 1–10 nm. Consequently, TEM micrographs confirmed that the mid-compositions had a dual-phase morphology with phase separation occurring on a 50–300 nm scale being present. The more extreme compositions had a clearly finer morphology with one dominant matrix with the polymer dispersed in it.

CONCLUSIONS

PUR/PEMA IPNs are semi-miscible over the entire composition range as seen from loss factor data. The mid-range compositions from 70% PUR to 40% PUR are slightly less miscible than the outer ranges with a shoulder for the second component being apparent. Phase domains in the OsO_4-stained TEM micrographs vary strongly with composition from 1 to 500 nm.

Three different morphology regimes, with dual-phase continuity only present at intermediate compositions, were found. A matrix of predominantly PUR with dispersed PEMA is believed to exist in the 90:10 and 80:20 PUR/PEMA compositions. At the 70:30 composition, a clear sign of change in phase continuity from a PUR matrix to a co-continuous morphology was observed from the modulus *versus* composition data and from the Shore A hardness values. Further, strong synergistic effects were found for the elongation at break and the toughness index at this composition. Dual-phase continuity was believed to extend over the intermediate compositions from 70:30 to 40:60. Here, properties such as the stress at break did not change dramatically and transmission electron micrographs also indicated two interconnected phases. At the lower end, from the 30:70 to 10:90 composition, a predominantly PEMA matrix with dissolved, discontinuous PUR was observed.

A new insight regarding modulus–composition studies has been gained. The temperature, at which the modulus values were taken, was seen to influence greatly the shape of the modulus–composition plot from Davies-like data to Budiansky-like data, indicating phase inversion at the mid-range composition. It was, therefore, suggested that in order to make such modulus–composition studies, modulus data should be taken at the intermediate temperature of the half-drop of the storage modulus curves of the PUR and PEMA homonetworks. Following this suggestion in the present study indicated that phase inversion took place at the 70:30 composition, which was in accordance with the findings from complementary experimental techniques.

ACKNOWLEDGEMENTS

The authors would like to acknowledge John Bates at Loughborough University for preparing the TEM micrographs. One of the authors (F.-U. S.) would like to acknowledge a grant from the German Academic Exchange Service, DAAD.

REFERENCES

1 Sperling, L. H. in 'Interpenetrating Polymer Networks', ACS 239 (Eds D. Klempner, L. H. Sperling and L. A. Utracki), American Chemical Society, Washington DC, 1994
2 Klempner, D. and Berkowski, L. in 'Encyclopedia of Polymer Science and Engineering' (Eds H. Mark, N. M. Bikales, C.G.O. Verberger and G. Menges), Vol. 8, Wiley, New York, 1988
3 Park, I. H., Lee, J. H. and Kim, S. C. *Polym. Bull.* 1983, **10,** 126
4 Huelck, V., Thomas, D. A. and Sperling, L. H. *Macromolecules* 1972, **5(4),** 340
5 An, J. H. and Sperling, L. H. in 'Cross-Linked Polymers', (Eds R. A. Dickie, S. S. Labana and R. S. Bauer), ACS Series 367, American Chemical Society, Washington DC, 1988
6 Hourston, D. J. and Schäfer, F.-U. *J. Polym. Adv. Technol.* 1996, **7,** 1
7 Donatelli, A. A., Sperling, L. H. and Thomas, D. A. *Macromolecules* 1976, **9,** 671, 676
8 He, X., Widmaier, J.-M. and Meyer, G. *Polym. Int.* 1993, **32,** 295

9 Akay, M. and Rollins, S. N. *Polymer* 1993, **34,** 1865
10 Allen, G., Boden, M. J., Todd, S. M., Blundell, D. J., Jeffs, G. M. and Davies, W. E. A. *Polymer* 1974, **15,** 28
11 Yeo, K. J., Sperling, L. H. and Thomas, D. A. *Polym. Eng. Sci.* 1981, **21(11),** 696
12 An, J. H., Fernandez, A. M. and Sperling, L. H. *Macromolecules* 1987, **20,** 191
13 Bauer, B. J. and Briber, R. M. in 'Advances in IPNs', (Eds D. Klempner and K. C. Frisch), Technomic Publishing, Lancaster, PA, 1994
14 Lipatov, Y., Shilov, S. V. V., Bogdanovic, V. A., Karabanova, L. V. and Sergeeva, L. M. *J. Polym. Sci., Polym. Phys. Edn* 1987, **25,** 43
15 Bauer, B. J., Briber, R. M. and Dickens, B. in 'Interpenetrating Polymer Networks', ACS 239 (Eds D. Klempner, L. H. Sperling and L. A. Utracki), American Chemical Society, Washington DC, 1994
16 Alig, I., Junker, M., Jenninger, W., Frisch, H. L. and Schulz, M. Conference Lecture, Morphology of Polymers, Prague, July 1995
17 Hourston, D. J. and Schäfer, F.-U. *High Perform. Polym.* 1996, **8,** 19
18 Ali, S. A. M. and Hourston, D. J. in 'Advances in Interpenetrating Polymer Networks' (Eds D. Klempner and K. C. Frisch), Vol. IV, Technomic Publishing Co. Inc., Lancaster, PA, 1994
19 Jordhamo, G. M., Manson, J. A. and Sperling, L. H. *Polym. Eng. Sci.* 1986, **26,** 517
20 Donatelli, A. A., Sperling, L. H. and Thomas, D. A. *J. Appl. Polym. Sci.* 1977, **21,** 1189
21 Sperling, L. H. 'Interpenetrating Polymer Networks and Related Materials', Plenum Press, New York, 1981
22 Mishra, V., Du Prez, F. and Sperling, L. H. *J. Polym. Mater. Sci. Eng.* 1995, **72,** 124
23 Tabka, M. T., Widmaier, J.-M. and Meyer, G. C. *Plastics, Rubber Comp. Process. Applic.* 1991, **16,** 11
24 Lee, D. and Kim, S. C. *Macromolecules* 1984, **17,** 268
25 Fox, T. G. *Bull. Am. Phys. Soc.* 1956, **1,** 123
26 Nielson, L. E. *J. Compos. Mater.* 1967, **1,** 100
27 Kerner, E. H. *Proc. Phys. Soc.* 1956, **B69,** 808
28 Davies, W. E. A. *J. Phys. D.* 1971, **4,** 1176
29 Davies, W. E. A. *J. Phys. D* 1971, **4,** 1325
30 Budiansky, B. *J. Mech. Phys. Solids* 1965, **13,** 223
31 Kim, S. C., Klempner, D., Frisch, K. C. and Frisch, H. L. *Macromolecules* 1977, **10,** 1187
32 Hourston, D. J. and Zia, Y. *J. Appl. Polym. Sci.* 1983, **28,** 3849
33 Hourston, D. J. and Zia, Y. *J. Appl. Polym. Sci.* 1983, **28,** 3745
34 Donatelli, A. A., Sperling, L. H. and Thomas, D. A. *Macromolecules* 1976, **9,** 4, 671
35 Nielson, L. E. *J. Appl. Polym. Sci.* 1977, **21,** 1579
36 Donnelly, P. I. 'Mechanical Properties of Polymers', Wiley-Interscience, New York, 1971
37 Nielson, L. E. 'Mechanical Properties of Polymers and Composites', Vol. 2, Marcel Dekker, New York, 1974
38 Technical literature, Operation instructions Zwick 3102, Zwick, D-7000 Ulm, Germany